The ROYAL COLLEGE of OPHTHALMOLOGISTS

ARTICLE

Check for updates

Baseline retinal vascular bed area on ultra-wide field fluorescein angiography correlates with the anatomical outcome of diabetic macular oedema to ranibizumab therapy: two-year analysis of the DAVE Study

Wenying Fan [1,2,3], Akihito Uji[2,3], Charles C. Wykoff[4,5], David M. Brown[4,5], Jano van Hemert [6], Khalil Ghasemi Falavarjani [2,3], Kang Wang[2,3], SriniVas R. Sadda[2,3] and Michael Ip[2,3 ✉]

PURPOSE: To determine the relationship between baseline retinal non-perfusion area (NPA) and retinal vascular bed area (RVBA) on ultra-wide field fluorescein angiography (UWF FA) and long-term response to intravitreal ranibizumab therapy in diabetic macular oedema (DMO).
METHODS: A post-hoc, 2-year observational case series. Baseline UWF FA images (Optos 200Tx) of 40 eyes from 29 patients with diabetes mellitus and treatment naïve DMO in the DAVE (NCT01552408) study were montaged and stereographically projected at the Doheny Image Reading Center to adjust for peripheral distortion. The retinal vasculature was automatically extracted to calculate RVBA. NPA was manually delineated by two masked certified graders. RVBA and NPA were computed in mm^2 automatically by adjusting for peripheral distortion and then correlated with the severity of DMO.
RESULTS: While global NPA at baseline was not correlated to retinal thickness measurements, baseline NPA in the superior retina was associated with the macular volume (MV) improvement ($P = 0.022$). Multivariate analysis revealed a smaller RVBA at baseline was correlated with a better MV outcome at two-year follow-up after adjusting for confounding factors ($P = 0.049$).
CONCLUSION: Eyes with smaller baseline RVBA appear to have a better long-term anatomic outcome of DMO.

INTRODUCTION

Diabetic macular oedema (DMO) is a major contributor of visual impairment in diabetic retinopathy (DR) [1] and occurs in 29% of individuals with diabetes for 20 years or more. [2] Although anti-vascular endothelial growth factor (VEGF) therapy for DMO has been shown to result in excellent visual outcomes [3, 4], not all eyes do well with therapy and repeat injections for recurrent DMO is required in many eyes; a baseline biomarker for predicting response to anti-VEGF therapy would be clinically important [5].

Prior studies on ultra-wide field (UWF) images suggest that retinal ischemia in the periphery may influence macular oedema (MO) in both retinal vein occlusion [6, 7] and DR. [8–10] Retinal non-perfusion area (NPA) is regarded as an indicator of retinal ischemia and is hypothesized to cause MO by triggering VEGF overexpression which may increase vascular permeability [1–9]. However, quantification of NPA on the entire retina has long been challenged by non-linear distortion when projecting the global retina to a 2D image [11, 12]. Instead, these studies expressed NPA in pixels or compared to the size of the optic disc (OD).

With the advent of the Optos 200Tx imaging system (Optos PLC, Dunfermline, Scotland), visualization of up to 200° of the retina within a single image is possible. Moreover, recent advances in UWF software enable the images at different gazes to be montaged together and the lesion size to be quantified in mm or mm^2 by correcting the non-linear distortion [13, 14]. Using this method, our prior study quantified NPA (mm^2) in treatment-naïve DMO on the montaged UWF fluorescein angiography (FA) but failed to find an association with the severity of DMO at baseline [15]. Nevertheless, there might be a potential time-window between the occurrence of non-perfusion and the expression of VEGF stimulated by ischemia. Thus, we proceeded with a longer-term observation to evaluate this hypothesis. As of yet, no prior observations have evaluated the influence of baseline retinal ischemia (non-perfusion) on UWF FA on the long-term response to anti-VEGF therapy.

Moreover, the advent of a new UWF algorithm enables a pan-retinal angiographic assessment. In the prior study, we used the term "retinal vascular bed area" (RVBA) to accurately indicate the projected area of vessels on fundus image [16]. After adjusting for the peripheral distortion on UWF FA, the total surface area of both

[1]Beijing Tongren Eye Center, Beijing Tongren Hospital, Beijing Ophthalmology and Visual Sciences Key Laboratory, Capital Medical University, Beijing, China. [2]Doheny Image Reading Center, Doheny Eye Institute, Los Angeles, CA, USA. [3]Department of Ophthalmology, David Geffen School of Medicine at UCLA, Los Angeles, CA, USA. [4]Retina Consultants of Houston, Houston, TX, USA. [5]Blanton Eye Institute, Houston Methodist Hospital & Weill Cornell Medical College, Houston, TX, USA. [6]Optos PLC, Dunfermline, UK. ✉email: ipmike333@gmail.com
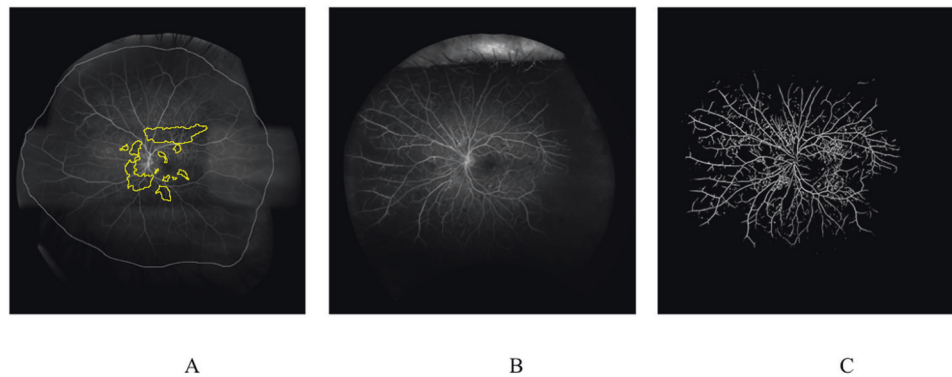
Fig. 1 **Total retinal area, non-perfusion area and segmentation of retinal vasculature on ultra-wide field fluorescein angiography (UWF FA). A** Total retinal area was defined as the total visible area of retina. Non-perfusion area was defined as the absence of retinal arterioles and/or capillaries. **B** Stereographically projected UWF FA image of eye with diabetic macular oedema. The early phase UWF FA frame right after the laminar venous phase was chosen to avoid the hyper-fluorescent foci due to the leakage of fluorescein dye and the obscuration of boundaries of the retinal vessels filled with fluorescein dye. On this frame both artery, capillary, and vein are well filled with dye with limited leakage. **C** Binarized imaging of retinal vasculature on Fig. 1B. Total area of white pixels was 64 mm^2.

arteries and veins bed, including both larger branches and smaller vessels could be precisely computed and expressed in mm^2 instead of using pixels (RVBA) [16]. Our prior analysis of the DAVE study already revealed an association between global RVBA and the severity of DMO at baseline [17]. The next step is to explore whether the baseline RVBA could influence or predict the long-term response of DMO to anti-VEGF therapy.

In this two-year follow-up, we aimed to explore the relationship of baseline NPA and RVBA (mm^2) quantified on UWF FA with the response to the anti-VEGF therapy for DMO after adjusting for confounding factors.

METHODS
Subjects
The DAVE study (ClinicalTrials.gov Identifier: NCT01552408) is a prospective, randomized, interventional clinical trial of patients with DMO aimed at comparing the efficacy and safety of ranibizumab monotherapy versus combination therapy of ranibizumab with UWF FA-guided retinal photocoagulation targeted to areas of capillary non-perfusion. All subjects signed a written informed consent and a Health Insurance Portability and Accountability Act (HIPAA) authorization. Inclusion criteria consisted of patients aged ≥18 years with DMO secondary to diabetes mellitus (DM) (Type 1 or 2). Participants had Early Treatment Diabetic Retinopathy Study (ETDRS) best-corrected visual acuity (BCVA) between 78 and 24 (Snellen equivalent, 20/32 to 20/320), with centre retinal thickness (CMT) ≥ 300 μm due to DMO measured by high definition spectral-domain optical coherence tomography (SD-OCT, Spectralis) on clinical examination. Decreased visual acuity (VA) was primarily the result of DMO, as determined by the subjective impression of the enrolling investigator. Clear ocular media and adequate pupillary dilatation to permit good quality fundus photography were required. Finally, baseline images from forty eyes of 29 patients with treatment naïve DMO were included in this analysis. None of the 40 eyes included had evidence of high myopia.

Image acquisition
The study protocol has been described in detail in the prior studies [15, 17–19]. Study eyes were dilated with tropicamide 1% and phenylephrine 2.5%, and UWF pseudocolour images were captured using the Optos 200Tx (Optos plc, Dunfermline, United Kingdom) centred on the fovea. After intravenous administration of fluorescein dye, UWF FA images were obtained during the early (45 s), middle (2 min and 30 s), and late (5 min) phases of the angiography, and steered peripherally (nasally, temporally, superiorly, and inferiorly).

Image projection and montage
Uncorrected raw images were collected and then sent to the Doheny Image Reading Center (Doheny Eye Institute, Los Angeles, California) for analysis. Images were transformed to stereographic projection images using proprietary prototype software available from the manufacturer. This projection technique was accomplished by ray tracing every pixel through a combined optical model of the Optos 200Tx and a Navarro UWF model eye with an axial length of 24 mm [20]. This optical model represented the projection used by the Optos 200Tx scanning laser ophthalmoscopy platform to create the two-dimensional Optomap. The software also allowed the grader to register the four steered images to the on-axis image automatically to create a montage of all images (by adding each image one by one). When the whole retina is not visible on one image, montaged image was created (Fig. 1A). Image registration between a pair of images first extracted their vasculature and subsequently applied rotational affine translation with cross-correlation (i.e., an algorithm slightly rotated the peripheral images to align vasculature). Finally, segments were blended together to create a contiguous montage.

Grading of retinal NPA and total retinal area
A region of non-perfusion was identified by the absence of retinal arterioles and/or capillaries with overall hypo-fluorescence relative to the overall background. The total retinal area (TRA) was defined as the total visible retina, allowing the ischemic index (ISI) to be calculated by dividing the NPA by the TRA.

Two masked, trained reading centre-certified UWF FA graders (K.W. and K.G.F.) independently analysed the image according to the previously reported standardized grading protocols. Graders were allowed to adjust the contrast and brightness to optimize visualization of the areas of nonperfusion. Using Image J version 1.49b (US National Institutes of Health, Bethesda, MD), the graders manually delineated the peripheral extent of the visible retina and the border of the NPA (Fig. 1A). Grading results were exported as binary mask and subsequently calculated in mm^2 automatically by summing the size of all pixels using software provided by the manufacturer (Optos plc). The size of a pixel was defined by its location in the image and was calculated using spherical trigonometry after projecting it back onto a sphere [19]. In case a difference in NPA, TRA, or ISI of >20% was present between graders, the graders met in open adjudication to agree on a single consensus result for each case. When smaller differences were present, the results of the two graders were averaged to yield a final result for subsequent correlative analyses.

Extraction and area measurement of retinal vasculature
The early UWF FA frame right after the laminar venous phase of the angiogram was selected to avoid hyper-fluorescent foci due to the leakage of fluorescein dye and the obscure boundaries of the retinal vessels filled with fluorescein dye. On this frame, both artery, capillary, and vein are well filled with fluorescent dye but with limited leakage. In addition, we also excluded the images if the retinal vessels were obscured by the background choroidal fluorescence, which makes it difficult to extract the vasculature because of a low contrast. Out of the 40 eyes in the DAVE study, binary images of retinal vasculature with sufficient quality were obtained in 25 eyes. Finally, baseline early-phase UWF FA images of 25 diabetic eyes were included in the analysis of retinal vasculature.

Table 1. Baseline demographic features of patients and study eyes with diabetic macular oedema.

Demographic features	Values
Baseline	
No. of eyes (No. of patients)	40 (29)
Age of first visit (years)	55.8 ± 9.5
Sex (male/female)	31/9
NPDR/PDR (No. of eyes)	34/6
Visual acuity	59.6 ± 13.2
HbA1c (%)	8.5 ± 2.1
DM duration (years)	12.6 ± 8.2
DMO duration (years)	2.0 ± 1.3
CMT (μm)	536.9 ± 192.8
MV (mm^3)	11.9 ± 2.7
Two-year follow-up	
Visual acuity	70.7 ± 13.5
CMT (μm)	320.3 ± 98.2
MV (mm^3)	9 ± 1.1
Mean number of injections per eye	17.9 ± 6.4
Panretinal photocoagulation (Yes/No)	20/20

Numeric data are presented as means ± standard deviation (SD).
NPDR non-proliferative diabetic retinopathy, *PDR* proliferative diabetic retinopathy, *HbA1c* glycosylated haemoglobin, *DM* diabetic mellitus, *DMO* diabetic macular oedema, *CMT* centre macular thickness, *MV* macular volume (mm^3).

The grayscale 2D UWF FA image was first converted to an 8-bit image (4000 × 4000 pixels). Using Image J, the image was converted into a binary version by a method consisting of three steps (Top-hat filter, Hessian filter, and Adaptive threshold). First, the image was processed using Top-hat filter with a window size of 12 pixels to remove the uneven illumination from the image. Then, Hessian filter and Adaptive threshold (median method) were used separately to create two binary images. Finally, two binary vessel imaging were combined to create the final copy by including the pixels detected both by those two methods (Hessian filter and Adaptive threshold) (Fig. 1B–C). The white pixels on the binary image represent retinal vasculature and were measured in mm^2 automatically. This method was reported by prior studies [21, 22].

To assess the repeatability of RVBA measurement on FA image, the frame right after the one chosen for vessel extraction was also selected and binarized. RVBA of those two early-phase frames but at different timing were compared. The result of the repeatability test was published in the prior study [17].

Distribution of retinal ischemia and RVBA
To assess the regional distribution of RVBA, NPA, and ISI, we took into account the nature of blood flow and divided retina into four quadrants centred on the centre of OD: supero-temporal, infero-temproal, supero-nasal, and infero-nasal quadrants.

Assessment of DMO
The presence and extent of DMO was evaluated by SD-OCT (Heidelberg Spectralis, Heidelberg Engineering, Germany) volume scans using a 20 × 20 degree (6 × 6 mm) scanning protocol with 512 A-scans and 496 B-scans (Automatic Real-Time level = 10). CMT was defined as the retinal thickness in the central subfield (central 1 mm). Macular volume (MV) was derived from entire 6x6mm volume. Both CMT and MV were obtained automatically by Heidelberg Eye Explorer software (Heidelberg Engineering GmbH; Version 1.9.10.0). Scans were inspected for segmentation errors, but as no significant (i.e., deviation of thickness boundary by more than 10% at any location) errors were detected, no manual correction was performed.

Statistical analysis
Statistical analysis was performed using the R statistical analysis package (version 3.3.0). Shapiro-Wilk normality test was used to explore the distribution normality of continuous variables. Homogeneity of variances was tested by the Bartlett test. Paired *T*-test or Wilcoxon signed-rank test was used to compare means at baseline with that in follow-up. For more than two groups, analysis of variance (ANOVA) or Kruskal–Wallis test (when ANOVA test not applicable) were performed. Univariate analysis was performed to explore the potential confounding factors and multivariate analysis was then used to evaluate the relationship of NPA or RBVA with the anatomical outcome (CMT or MV) of DMO at two-year follow-up. Generalized estimating equations (GEE) was used to adjust for interactions between two eyes of the same patient. Statistical results were expressed as *P* values. A *P*-value of <0.05 was considered statistically significant.

RESULTS
Baseline demographic features, retinal NPA (ischemic index) and RVBA on UWF fluorescein angiography
A total of 40 eyes from 29 patients (6 proliferative DR: PDR; 34 non-proliferative DR: NPDR) with treatment naïve DMO were included in the analysis. Demographic features were listed in Table 1, with a global RVBA of 54.7 ± 16.6 mm^2 and NPA of 196.1 ± 123.4 mm^2 (ISI: 0.31 ± 0.2) at baseline [17]. The distribution of RVBA and NPA at baseline on UWF FA were described in detail in the prior study [17].

Visual and anatomical outcomes at 2-year follow-up
Visual and anatomical outcomes at two-year follow-up was presented in Table 1. Mean VA was increased from 59.6 ± 13.2 EDTRS letters to 70.7 ± 13.5 in two-year follow-up (*P* < 0.001), with mean reduction of CMT from 536.9 ± 192.8 μm to 320.3 ± 98.2 (*P* < 0.001) and mean improvement of MV from 11.9 ± 2.7 mm^3 to 9 ± 1.1 (*P* < 0.001) (Table 1). Mean number of injections was 17.9 ± 6.4 and 20 eyes received retinal photocoagulation. At the 2-year follow-up, VA was correlated with MV (*R* = −0.44, *P* = 0.026) but not CMT (*R* = −0.23, *P* = 0.201).

Association between baseline demographic features and the prognosis of DMO at the 2-year follow-up
The number of injections was related to CMT (*P* = 0.001, Table 2) and MV (*P* < 0.001, Table 2) improvement and retinal photocoagulation was associated with MV response (*P* = 0.003, Table 2). The baseline level of glycosylated haemoglobin (HbA1c) correlated with MV outcome (*P* < 0.001, Table 2). No relationship was observed of DMO prognosis (CMT or MV) with age, sex, baseline VA, diabetic duration, DMO duration, and baseline CMT or MV (*P* > 0.05).

Association of baseline RVBA and NPA with the prognosis of DMO in 2-year follow-up
Global RVBA at baseline was significantly associated with MV improvement in two-year follow-up (*R* = 0.49, *P* = 0.04, Table 3), and the association was also present in the infero-temproal and supero-nasal quadrants, superior and inferior retina, respectively (*P* < 0.05, Table 3). No association was observed between baseline RVBA and CMT improvement (*P* > 0.05).

No significant correlation of global NPA (or ISI) at baseline was observed with CMT or MV in two-year follow-up (*P* > 0.05, Table 4). However, NPA in superior quadrant was correlated with MV improvement (*R* = 0.36, *P* = 0.022, Table 4).

After adjusting for the confounding factors identified in the univariate analyses (the number of injection, retinal photocoagulation and the level of HbA1c), multivariate analysis revealed a significant association between baseline RVBA and MV at two-year follow-up (*P* = 0.049).

DISCUSSION
In this cohort followed for two-years, we explored the association between NPA or RVBA (mm^2) on UWF FA at baseline and the response to ranibizumab therapy in DMO. Multivariate analysis revealed that a smaller global RVBA at baseline was an

Table 2. Association between baseline biomarkers and retinal thickness measurements at 2-year follow-up.

Baseline demographic features	2-year follow-up			
	CMT		MV	
	R	P	R	P
Age of first visit (years)	0.3	0.067	−0.13	0.492
Sex (male/female)	0.16	0.209	−0.09	0.25
Baseline visual acuity	0.06	0.739	0.0046	0.149
CMT (μm)	0.04	0.822	0.04	0.628
MV (mm³)	−0.04	0.859	0.16	0.481
HbA1c (%)	−0.16	0.191	0.27	<0.001
DM duration (years)	0.07	0.754	−0.04	0.989
DMO duration (years)	0.12	0.472	0.01	0.933
No. of injection	0.45	0.001	0.14	<0.001
Retinal photocoagulation (yes/no)	0.2	0.113	0.33	0.003
Baseline RVBA	0.12	0.779	0.49	0.04
Baseline NPA	0.03	0.828	0.31	0.066
Baseline ISI	−0.0008	0.956	0.28	0.162

Linear modelling was applied to calculate Pearson correlation coefficient. Generalized estimating equations (GEE) was used to adjust for interactions between two eyes of the same patient.
CMT centre macular thickness, MV macular volume (mm³), HbA1c glycosylated haemoglobin, DM diabetic mellitus, DMO diabetic macular oedema, RVBA retinal vascular bed area, NPA non-perfusion area, ISI ischemic index.
Values of P (two-tailed) <0.05 was considered statistically significant.

Table 3. Correlation of baseline retinal vascular bed area with the severity of diabetic macular oedema at 2-year follow-up.

Baseline RVBA	CMT		MV	
	R	P	R	P
Whole fundus	0.12	0.779	0.49	0.04
Supero-temporal quadrant	−0.07	0.483	0.278	0.146
Infero-temproal quadrant	0.15	0.712	0.492	0.022
Supero-nasal quadrant	0.18	0.594	0.474	0.024
Infero-nasal quadrant	0.15	0.553	0.279	0.275
Temporal hemisphere	0.06	0.963	0.477	0.051
Nasal hemisphere	0.18	0.554	0.416	0.093
Superior hemisphere	0.05	0.88	0.399	0.021
Inferior hemisphere	0.16	0.645	0.436	0.039

Generalized estimating equations (GEE) was used to adjust for interactions between two eyes of the same patient.
RVBA retinal vascular bed area, CMT centre macular thickness, MV macular volume (mm³).
Values of P (two-tailed) <0.05 was considered statistically significant.

Table 4. Correlation of baseline non-perfusion area and ischemic index with the severity of diabetic macular oedema at 2-year follow-up.

	Linear correlation			
	CMT		MV	
	R	P	R	P
NPA				
Whole	0.03	0.828	0.31	0.066
Supero-temporal	0.15	0.399	0.3	0.095
Infero-temproal	0.15	0.401	0.3	0.111
Supero-nasal	−0.07	0.626	0.36	0.07
Infero-nasal	−0.21	0.173	0.01	0.929
Temporal	0.16	0.406	0.33	0.05
Nasal	−0.15	0.26	0.22	0.283
Superior	0.05	0.704	0.36	0.022
Inferior	−0.01	0.998	0.2	0.287
ISI				
Whole	−0.0008	0.956	0.28	0.162
Supero-temporal	0.17	0.266	0.35	0.07
Infero-temproal	0.08	0.468	0.27	0.199
Supero-nasal	−0.08	0.563	0.26	0.155
Infero-nasal	−0.28	0.065	−0.09	0.4
Temporal	0.14	0.342	0.34	0.078
Nasal	−0.18	0.13	0.11	0.92
Superior	0.07	0.638	0.34	0.05
Inferior	−0.08	0.626	0.16	0.776

Generalized estimating equations (GEE) was used to adjust for interactions between two eyes of the same patient.
CMT centre macular thickness, MV macular volume (mm³), NPA non-perfusion area, ISI ischemia index.
Values of P (two-tailed) <0.05 was considered statistically significant.

independent predictor for a better MV response after adjusting for confounding factors. In contrast, global NPA at baseline was not associated with either CMT or MV improvement. A marginal association was observed between baseline NPA in the superior retina and MV improvement.

Michael et al. quantified the leakage of microaneurysms (MA) using semi-automated segmentation of FA and found anti-VEGF treatment for DMO results in decreased diffuse leakage as assessed on FA [23]. However, as we know, the leakage of fluorescence dye changes dynamically with an un-distinguished border. Thus, quantification of the leakage was limited by inherent subjectivity and challenges in reproducibility. It may be better to attempt to quantify the anatomical basis of fluid leakage or exudation, e.g., RVBA. In essence, RVBA contained two important vessel variables (diameter and length) and thus can indicate the changes of retinal vascular bed which is thought to be the primary pathologies in a set of retinal vascular disorders.

In our prior cross-sectional study at baseline, we demonstrated a reliable measurement of RVBA in mm² on the UWF FA image [17]. RVBA was observed to increase in eyes with DMO compared with age and sex-matched healthy controls, and also correlated with the severity of DMO. In the present study, we also observed that a smaller RVBA at baseline was correlated with a better MV outcome at the two-year follow-up. An increased RVBA may indicate an expanded retinal vascular bed caused by a dilation or elongation of vessels or both, which provides the anatomic basis for the iBRB breakdown and fluid leakage outward from the vessels. Supportively, a series of studies revealed an association between the presence, development or reduction of DMO with vascular morphologic changes. Kristinsson et al. found a significant dilatation and elongation of retinal vessels was present before the diagnosis of DMO [24]. Moreover, the 6-year incidence in DMO was found to be 11% and associated with an increase of 10 μm in centre retinal vein equivalents even after adjusting for the duration, diabetes type, and other factors [25]. Kurt et al. found that both a single injection of intravitreal ranibizumab or bevacizumab in eyes with DMO significantly constricted the retinal blood vessel diameters [26]. Moreover, in a combined

cohort of DAVE and RECOVERY study (ClinicalTrials.gov Identifier: NCT02863354), we further found that RVBA was also correlated with the severity of DR (under review). The association between RVBA and disease severity may help explain why the original RVBA differences continue to correlate with the anatomical response, even after two years of therapy. In addition, we observed that this association was also present in the temporal retina, which is similar to the prior observation at baseline that the association between RVBA and DMO was more significant in the temporal retina. This could be explained by the fact that diabetic lesions tend to preferably involve the temporal retina [27, 28]. These findings suggested a combined effect on both lesion size and its distribution on the severity of DMO.

Retinal ischemia has long been hypothesized to correlate with DMO by triggering VEGF overexpression. However, our prior study failed to find the association between NPA (mm^2) and the severity of DMO at baseline [15]. Consistently, no association was observed in this two-year observation. Using a similar method, Silva et al. also failed to find an association between retinal ischemia and DMO [29]. Interestingly, despite a lack of association globally, a marginal association was present at the superior retina. In normal subjects, the outer border of the retina was defined as the junction between the vascularized and non-vascularized retina by our group [13]. This method provides a useful reference when calculating NPA at the far-periphery and ISI. However, in some diseased conditions like DR, the peripheral segment of the blood vessel may be nonperfused and make it difficult to determine the original physiologic outer border of vasculature. Therefore, errors may be incurred in the quantification of the peripheral NPA or ISI, even with a small deviation due to a relatively far distance from the fovea. We noticed that, aside from the superior region, the statistical associations appeared to be marginal both temporally and for the entire retina as well. It may be reasonable to expect a significant association if future adjustments and/or improvement in the quantification of NPA can be achieved.

The current study has some strengths. First, the DAVE study is a well-designed, multicentre and prospective clinical study, and all the cases had both high-quality OCT at baseline and follow-up. Second, FA provided superior resolution of the crucially important microvasculature in comparison with fundus images and the measures of RVBA on early-phase of FA demonstrated a good repeatability in our prior study. Third, the NPA grading was performed by two masked and experienced graders at the Doheny Image Reading Center using a standard protocol. Lastly, images were all stereographic projected and distortion corrected, and both the RVBA and NPA were expressed in mm^2 rather than in pixels for the first time.

The present study is not without limitation. The peripheral distortion was corrected by hypothesizing that the model axial length is 24 mm; lacking an exact axial length for each case may lead to measurement error. However, none of the enrolled patients had high myopia. Another limitation is that while the source of the data is from a prospective study with standardized UWF FA acquisition protocol, the analyses presented in this report are post-hoc. Moreover, since the DAVE was study was a 3-year observation, an ending point analysis is needed to verify our findings in the future. Finally, the present study is inevitably limited by its small sample size. This methodology study introduced a novel biomarker that needs further evaluation in the future. However, differing from the traditional ETDRS scale system which is time-consuming and labouring, RVBA is a novel biomarker that could be precisely semi-automated computed to reflect the vascular changes for the entire retina on UWF FA. Our findings need be to further verified in a larger cohort of eyes that have had UWF-FA performed and then graded in a standardized fashion.

In summary, we observed that baseline RVBA was correlated with the long-term anatomical outcome of DMO receiving anti-VEGF therapy after adjusting for confounding factors.

Summary
What was known before

- Retinal vascular bed area (RVBA) is a novel biomarker which could be precisely computed in mm^2 by correcting distortion on UWF FA.

What this study adds

- The present study observed that baseline retinal vascular bed area (mm^2) was an independent predictor for the long-term anatomical outcome of diabetic macular oedema receiving anti-vascular endothelial growth factor therapy.

REFERENCES

1. Romero-Aroca P, Baget-Bernaldiz M, Pareja-Rios A, Lopez-Galvez M, Navarro-Gil R, Verges R. Diabetic macular edema pathophysiology: vasogenic versus inflammatory. J Diabetes Res. 2016;2016:2156273.
2. Klein R, Knudtson MD, Lee KE, Gangnon R, Klein BEK. The Wisconsin Epidemiologic Study of Diabetic Retinopathy XXIII: the twenty-five-year incidence of macular edema in persons with type 1 diabetes. Ophthalmology. 2009;116:497–503.
3. Dervenis N, Mikropoulou AM, Tranos P, Dervenis P. Ranibizumab in the Treatment of Diabetic Macular Edema: A Review of the Current Status, Unmet Needs, and Emerging Challenges. Adv Ther. 2017;34:1270–82.
4. Singer MA, Kermany DS, Waters J, Jansen ME, Tyler L. Diabetic macular edema: it is more than just VEGF. F1000Research. 2016;5.
5. Stewart MW. Anti-VEGF therapy for diabetic macular edema. Curr Diab Rep. 2014;14:510.
6. Singer M, Tan CS, Bell D, Sadda SR. Area of peripheral retinal nonperfusion and treatment response in branch and central retinal vein occlusion. Retina. 2014;34:1736–42.
7. Abri Aghdam K, Reznicek L, Soltan Sanjari M, Klingenstein A, Kernt M, Seidensticker F. Anti-VEGF treatment and peripheral retinal nonperfusion in patients with central retinal vein occlusion. Clin Ophthalmol. 2017;11:331–6.
8. Patel RD, Messner LV, Teitelbaum B, Michel KA, Hariprasad SM. Characterization of ischemic index using ultra-widefield fluorescein angiography in patients with focal and diffuse recalcitrant diabetic macular edema. Am J Ophthalmol. 2013;155:1038–44. e2.
9. Wessel MM, Nair N, Aaker GD, Ehrlich JR, D'Amico DJ, Kiss S. Peripheral retinal ischaemia, as evaluated by ultra-widefield fluorescein angiography, is associated with diabetic macular oedema. Br J Ophthalmol. 2012;96:694–8.
10. Rabiolo A, Parravano M, Querques L, Cicinelli MV, Carnevali A, Sacconi R, et al. Ultra-wide-field fluorescein angiography in diabetic retinopathy: a narrative review. Clin Ophthalmol. 2017;11:803–7.
11. Kim JH, Jung H-G, Chung HJ, Lee K, Sohn J. Simplified correction of ischemic index in diabetic retinopathy evaluated by ultra-widefield fluorescein angiography. Korean J Ophthalmol. 2015;29:168–72.
12. Oishi A, Hidaka J, Yoshimura N. Quantification of the image obtained with a wide-field scanning ophthalmoscope. Invest Ophthalmol Vis Sci. 2014;55:2424–31.
13. Singer M, Sagong M, van Hemert J, Kuehlewein L, Bell D, Sadda SR. Ultra-widefield imaging of the peripheral retinal vasculature in normal subjects. Ophthalmology. 2016;123:1053–9.
14. Croft DE, van Hemert J, Wykoff CC, Clifton D, Verhoek M, Fleming A, et al. Precise montaging and metric quantification of retinal surface area from ultra-widefield fundus photography and fluorescein angiography. Ophthalmic Surg Lasers Imaging Retina. 2014;45:312–7.
15. Fan W, Wang K, Ghasemi Falavarjani K, Sagong M, Uji A, Ip M, et al. Distribution of Nonperfusion Area on Ultra-widefield Fluorescein Angiography in Eyes With Diabetic Macular Edema: DAVE Study. Am J Ophthalmol. 2017;180:110–6.
16. Fan W, Uji A, Borrelli E, Singer M, Sagong M, van Hemert J, et al. Precise measurement of retinal vascular bed area and density on ultra-wide fluorescein angiography in normal subjects. Am J Ophthalmol. 2018;188:155–63.

17. Fan W, Uji A, Wang K, Falavarjani KG, Wykoff CC, Brown DM, et al. Severity of diabetic macular edema correlates with retinal vascular bed area on ultra-wide field fluorescein angiography: DAVE Study. Retina. 2020;40:1029–37.

18. Tan CS, Chew MC, van Hemert J, Singer MA, Bell D, Sadda SR. Measuring the precise area of peripheral retinal non-perfusion using ultra-widefield imaging and its correlation with the ischaemic index. Br J Ophthalmol. 2016;100:235–9.

19. Sagong M, van Hemert J, Olmos de Koo LC, Barnett C, Sadda SR. Assessment of accuracy and precision of quantification of ultra-widefield images. Ophthalmology. 2015;122:864–6.

20. Escudero-Sanz I, Navarro R. Off-axis aberrations of a wide-angle schematic eye model. J Opt Soc Am A Opt Image Sci Vis. 1999;16:1881–91.

21. Kim AY, Chu Z, Shahidzadeh A, Wang RK, Puliafito CA, Kashani AH. Quantifying microvascular density and morphology in diabetic retinopathy using spectral-domain optical coherence tomography angiography. Invest Ophthalmol Vis Sci. 2016;57:OCT362–70.

22. Uji A, Balasubramanian S, Lei J, Baghdasaryan E, Al-Sheikh M, Sadda SR. Impact of multiple En face image averaging on quantitative assessment from optical coherence tomography angiography images. Ophthalmology. 2017;124:944–52.

23. Allingham MJ, Mukherjee D, Lally EB, Rabbani H, Mettu PS, Cousins SW, et al. A quantitative approach to predict differential effects of Anti-VEGF treatment on diffuse and focal leakage in patients with diabetic macular edema: a pilot study. Transl Vis Sci Technol. 2017;6:7.

24. Kristinsson JK, Gottfredsdóttir MS, Stefánsson E. Retinal vessel dilatation and elongation precedes diabetic macular oedema. Br J Ophthalmol. 1997;81:274–8.

25. Klein R, Myers CE, Lee KE, Gangnon R, Klein BEK. Changes in retinal vessel diameter and incidence and progression of diabetic retinopathy. Arch Ophthalmol (Chic, Ill 1960). 2012;130:749–55.

26. Kurt MM, Çekiç O, Akpolat Ç, Elçioglu M. Effects of intravitreal ranibizumab and bevacizumab on the retinal vessel size in diabetic macular edema. Retina. 2018;38:1120–26.

27. Silva PS, Cavallerano JD, Sun JK, Soliman AZ, Aiello LM, Aiello LP. Peripheral lesions identified by mydriatic ultrawide field imaging: distribution and potential impact on diabetic retinopathy severity. Ophthalmology. 2013;120:2587–95.

28. Haj Najeeb B, Simader C, Deak G, Vass C, Gamper J, Montuoro A, et al. The distribution of leakage on fluorescein angiography in diabetic macular edema: a new approach to its etiology. Invest Ophthalmol Vis Sci. 2017;58:3986–90.

29. Silva PS, Dela Cruz AJ, Ledesma MG, van Hemert J, Radwan A, Cavallerano JD, et al. Diabetic retinopathy severity and peripheral lesions are associated with nonperfusion on ultrawide field angiography. Ophthalmology 2015;122:2465–72.

AUTHOR CONTRIBUTIONS

FUNDING

COMPETING INTERESTS

The authors declare no competing interests.

ADDITIONAL INFORMATION

Correspondence and requests for materials should be addressed to Michael Ip.

Reprints and permission information is available at http://www.nature.com/reprints

Publisher's note Springer Nature remains neutral with regard to jurisdictional claims in published maps and institutional affiliations.